VTT Technical Research Centre of Finland

Failure analysis of duplex 2205 gas separator welds

Nevasmaa, Pekka; Yli-Olli, Sanni

Published in:
BALTICA XI 2019

Published: 01/01/2019

Document Version
Publisher's final version

Failure analysis of duplex 2205 gas separator welds

Pekka Nevasmaa[1] & Sanni Yli-Olli[1]

[1]VTT Technical Research Centre of Finland Ltd
Espoo, Finland

Abstract

In a shutdown of a refinery, extensive cracks parallel to a circumferential butt-welded joint were found in a gas separator made of 2205 duplex stainless steel (22%Cr–5%Ni–3%Mo). The welded joint detail had been in service for about two years under conditions involving 45 °C max internal temperature and 47 bar internal pressure in a mixture of hydrogen, hydrogen sulphide, carbon dioxide and water. The objective was to characterise the mechanisms and underlying causes of cracking.

In microscopic and fractographic investigations, the cracks exhibited features pointing to initiation promoted by local anomalous regions within a thin layer next to the plate surface and close to several surface cracks. Within this layer, precipitates in the ferrite phase formed an intragranular 'peppery' structure. The layer exhibited hardness higher than in ferrite or austenite phases alone. These findings suggest that the layer contains precipitates of chromium nitride, Cr_2N. Such precipitates have been attributed to an increased susceptibility to hydrogen embrittlement and reduced resistance of duplex steel to hydrogen-induced stress cracking (HISC). Several microstructural and fractographic details characteristic of the HISC mechanism were identified. In spite of the complexities of the surface anomalies extending to base material, the 'rough' surface was accompanied by coarsened HAZ-resembling microstructure, suggesting that it originated from an accidental thermal treatment, such as plasma cutting or flame straightening. Local areas with striations on the crack fracture surface were attributed to fatigue at later stages of crack propagation. It was concluded that the observed cracking was due to a combination of (i) initiation and propagation by hydrogen-induced stress cracking (HISC) and (ii) later propagation by fatigue.

1. Introduction

Duplex stainless steels (DSS) are often used in oil & gas industry, refining & process industry and chemical tankers in constructions operating in demanding conditions that require a combination of high strength ($R_{p0.2}$ > 425 MPa) and good corrosion resistance. DSS also exhibit adequate toughness properties in the -40…+280 °C temperature range [1]. The nominal [2,3] and actual chemical compositions of the investigated DSS grade 2205 (EN 1.4462) are given in Table 1.

Duplex stainless steels have a two-phase microstructure consisting of approx. 50% ferrite and 50% austenite. DSS have higher chromium contents, as compared to common austenitic stainless steel grades, and owing to the Mo and N alloying, they typically present a higher resistance to chloride pitting corrosion and crevice corrosion, compared to austenitic grades SS 304L and SS 316L [2]. In addition, DSS generally exhibit a better resistance to chloride stress corrosion cracking (Cl-SCC); therefore, they are often used as replacement materials for more conventional SS 300 series stainless steels. Nonetheless, DSS are not immune to Cl-SCC and their resistance may be affected by environmental factors, e.g. boiling on the surface

causing chloride concentration and hydrogen sulphide interactions increasing cracking susceptibility [2]. In addition to Cl-SCC, these alloys may be susceptible to environmental hydrogen assisted cracking mechanisms, such as hydrogen stress cracking and hydrogen induced cracking, as well as precipitation of brittle metallic phases at elevated operation temperatures [1–3]. Thus, DSS are traditionally not suitable for use at temperatures above 280–300 °C due to increasing susceptibility to thermal embrittlement because of brittle phase precipitation, after exposure to elevated temperatures [1,2].

Table 1. Nominal and actual chemical composition (w-%) for duplex stainless steel grade 2205 (EN 1.4462) – nominal [2, 3]: former row; analysed: latter row.

Element / w-%	**Nominal and actual chemical composition (%)**										
	C	Si	Mn	P	S	Cr	Ni	Mo	N	Cu	W
	.020–.030	1.0	2.0	.030	.020	22–23	5.3–5.7	2.8–3.2	0.12–0.18	-	-
	.024	.45	1.68	.030	.002	22.5	5.47	3.09	0.17	.10	.02

Overall, modern duplex stainless steels have good weldability. Most problems are commonly encountered when either too low or excessively high heat input is used, when dilution is too high and when too much nitrogen is lost from the weld pool [3]. Too rapid weld cooling rates associated with low heat inputs often result in excessively high ferrite content and pronounced chromium nitride precipitation, which easily impairs corrosion resistance and toughness properties [1,3]. High heat input or repeated heating to approx. 600–1000 °C temperature range (e.g. multiple-pass welding) may result in excessively high austenite content and formation of intermetallic phases, although the latter is more of a problem with higher-alloyed DSS grades [3]. For the 2205 grade, a recommended arc energy range is around 0.5–2.5 kJ/mm, depending on the welding process and section thickness [3,4]. Preheating is usually not required, with the exception for heavily restrained joints where preheating up to max. 150 °C can be used to minimize the cracking risk [3]. Apart from solution annealing, post-weld heat treatments are not recommended due to a risk of high-temperature embrittlement [3]. For the same reason, the maximum interpass temperature during multipass welding of 2205 grade should be limited to 250 °C [4].

For the 2205 grade (EN 1.4462), 'matching' filler materials such as 22Cr–9Ni–3Mo+N boosted with nickel are generally used. For repair welding or on-site assembly welds, austenitic E 309 MoL filler metal can also be applied. With 'matching' filler materials, the molten weld metal in DSS is more sluggish than with austenitic stainless steel; consequently, weld penetration can easily remain incomplete unless the welding parameters are carefully optimised [4]. The use of slightly wider root gap, smaller root face and a groove angle about 10° larger than for standard stainless steel joints, are therefore generally recommended [3,4]. The risk of unmelted joint corner due to incomplete weld penetration is faced particularly with T-joint fillet welds.

Although duplex stainless steels are considered resistant to hydrogen-induced cracking during welding, failures have occurred in weldments due to a combination of high hydrogen contents and unsuccessful microstructure control [1]. These cracking incidents are usually associated with excessively high ferrite content (i.e., FN > 80) in conjunction with the presence of sufficient hydrogen and high stress e.g. due to heavily restrained weldments and structures of high rigidity [1,3,4].

2. Background and Methods

Extensive crack-like defects in a DSS 2205 gas separator discovered during a shutdown of a refinery were located close to circumferential butt-welded joint connecting different parts of the separator (Figure 1). The butt-welded joint detail in the gas separator had been in use for approx. 2 years in refinery service conditions involving a 45 °C maximum internal usage temperature, 47 bar internal operational pressure and a mixture of hydrogen, hydrogen sulphide (≈170–500 vol-ppm), carbon dioxide, water and small amount of carbon monoxide (0.3–0.4 mol-%) as contents inside the separator. After about 2 years in service, the investigated joint detail was found to reveal comparatively long crack-like defects close to a circumferential butt-welded joint and running parallel to the weld. Welding had been carried out according to appropriate WPSs using 'matching' 22%Cr–9%Ni grade duplex filler metal over-alloyed with nickel.

The objective of the failure investigation was to characterise the fracture micromechanism associated with the gas separator failure in order to identify the underlying causes of occurrence of failure.

Figure 1. Cross section sample from a cracked detail: crack initiation at the plate surface close to the weld (left), crack propagation nearly through the entire section thickness, with occasional crack branching.

The specimens extracted from the damaged gas separator were subjected to the following investigations:

(i) Visual inspection and documentation of the observed damages.

(ii) Chemical analysis of the gas separator material using optical emission spectroscopy (OES).

(iii) Optical microscopy (LOM) of the gas separator material using polished and etched cross section samples (in relation to the circumferential butt-weld): characterisation of microstructural features and ferrite-austenite balance, detection and identification of precipitates, inclusions, segregations, metallic phases, etc. Etching was performed using oxalic acid electrolytic etch followed by NaOH electrolytic etch.

(iv) Scanning electron microscopy (SEM) with energy dispersive X-ray spectroscopy analysis (EDS): fractographic investigation of opened, authentic crack fracture surfaces, identification of fracture micromechanism, analysis of elements on the fractured surface, identification of microcracks.

(v) Microhardness measurements of the gas separator material: through-thickness measurements of next-to-surface area and both phases (ferrite, austenite) using Vickers $HV_{0.1}$.

3. Results

Results of the metallographic and fractographic investigations of the examined cracked samples extracted from the damaged gas separator specimens are presented in the following.

3.1 Visual examination

It was recognised that more or less continuous crack-like defects were running circumferentially, parallel to butt-weld, within varying distance from the weld. Occasionally, the cracks located at the immediate vicinity of the fusion boundary; at some locations, they ran further away in the outer heat-affected zone (HAZ).

Additionally, the welded sides of samples cut along the weld centerline revealed internal volumetric imperfections and defects within the weld metal close to the weld centre region in the plate thickness direction (c.f. Figure 1). These imperfections imply that welding of the weld root region, in this respect, had technically failed, which, in turn, had prevented achieving a sound weld root and hence resulted in poor weld quality.

3.2 Fractographic investigation

The results of the fractographic investigation using scanning electron microscopy (SEM) with energy dispersive X-ray spectroscopy analysis (EDS) are shown in Figures 2–5. The fracture surface had two different types of dominating areas. The first type was relatively flat showing several side cracks with random orientation, as well as ridges and very few striations and “feathery” like fracture propagation (Figures 2, 4 and 5). The second areas were smaller and revealed often relatively steep level changes between the flat areas, showing dimples and more ductile fracture propagation (Figure 3).

No traces of environmental contamination within the cracks were found in the EDS analysis.

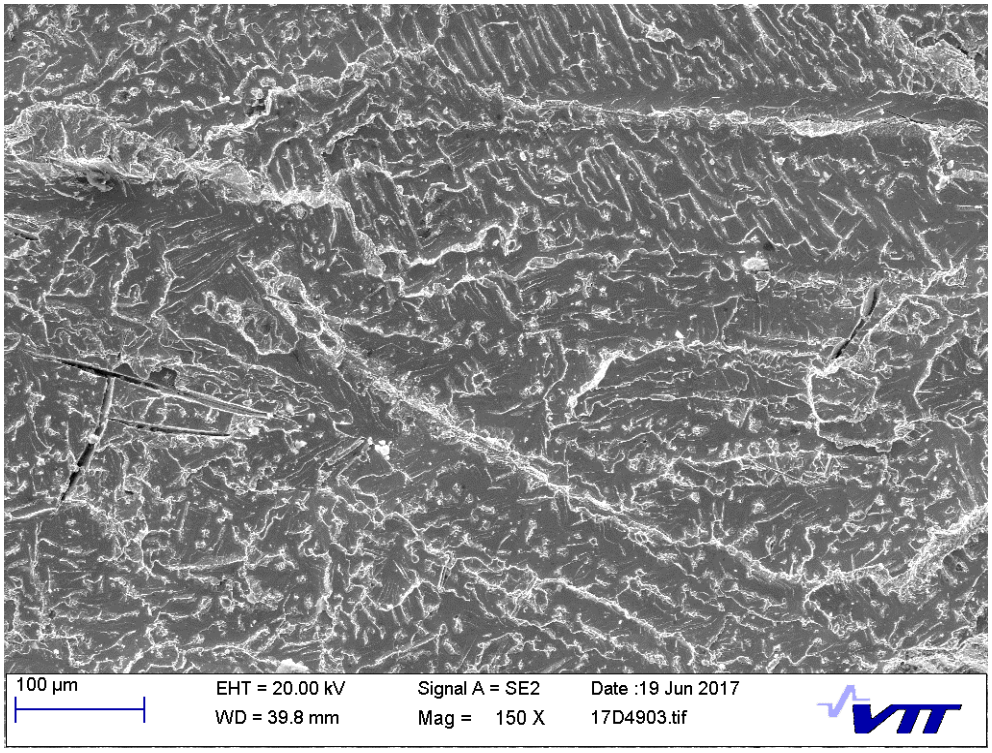

a)

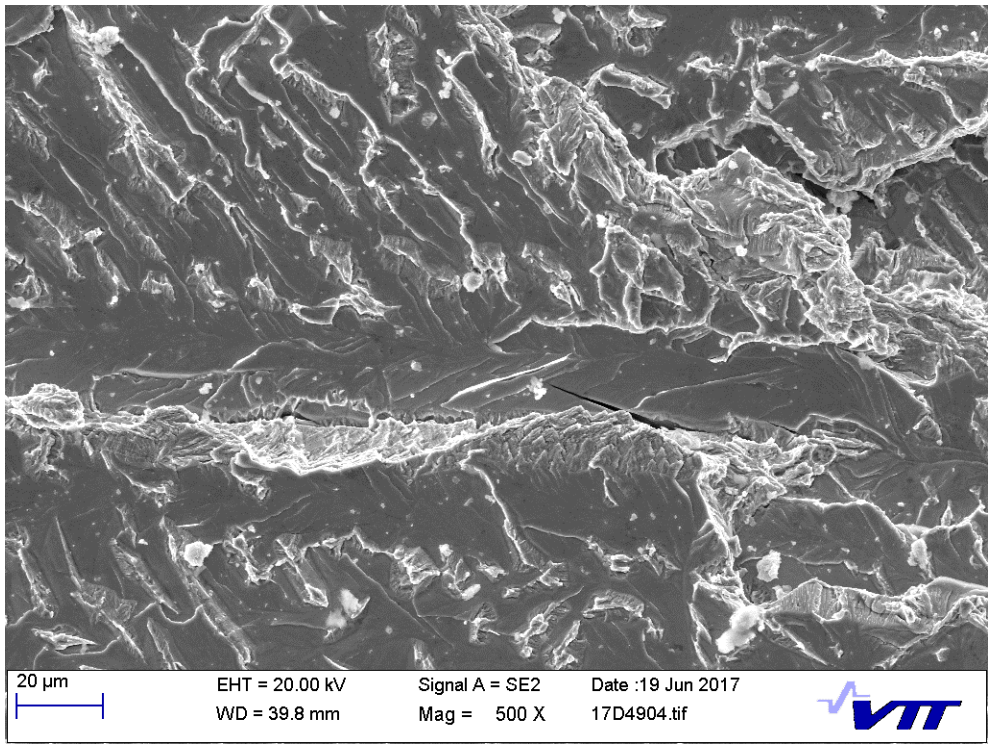

b)

Figure 2. Fracture surface near the plate outer surface, showing “flat” fracture and side cracks. (a) Outer surface on top, fracture propagation from top to bottom; (b) detail of the fracture surface in (a).

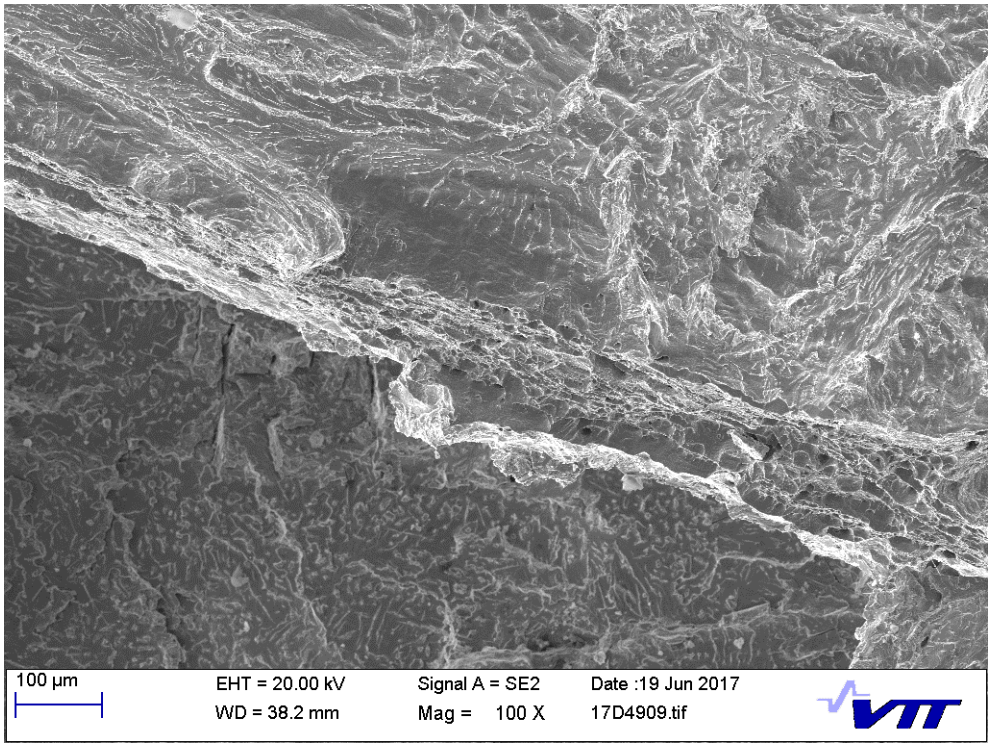

a)

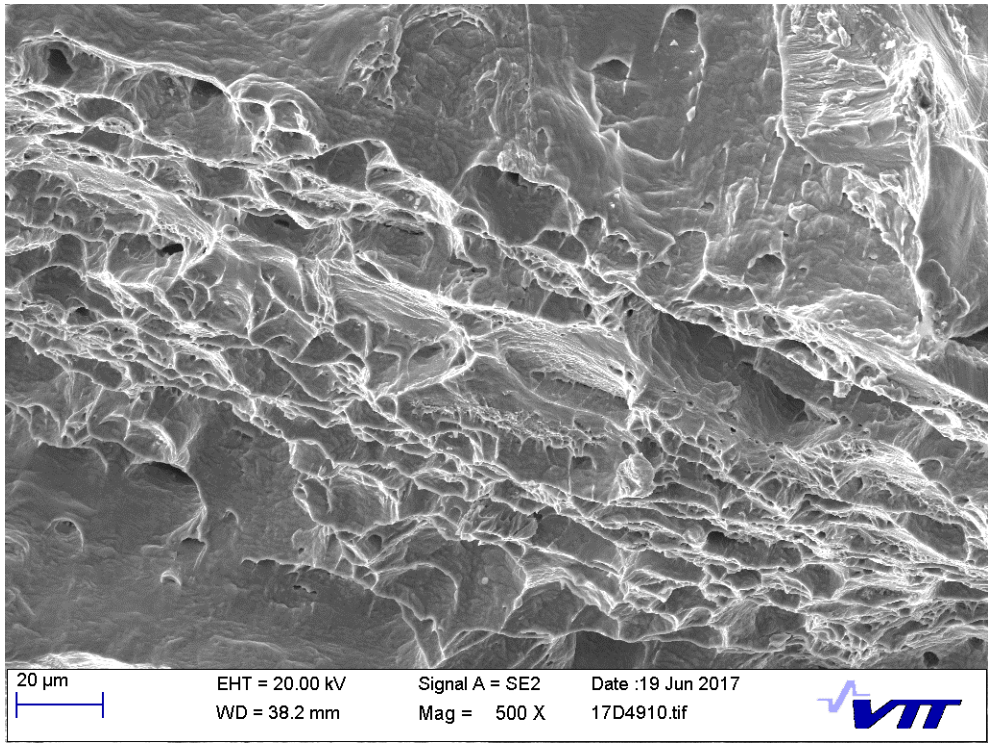

b)

Figure 3. Fracture surface from the middle of the sample, showing level changes and dimples. (a) Outer surface on top, fracture propagation from top to bottom; (b) detail of the fracture surface in (a).

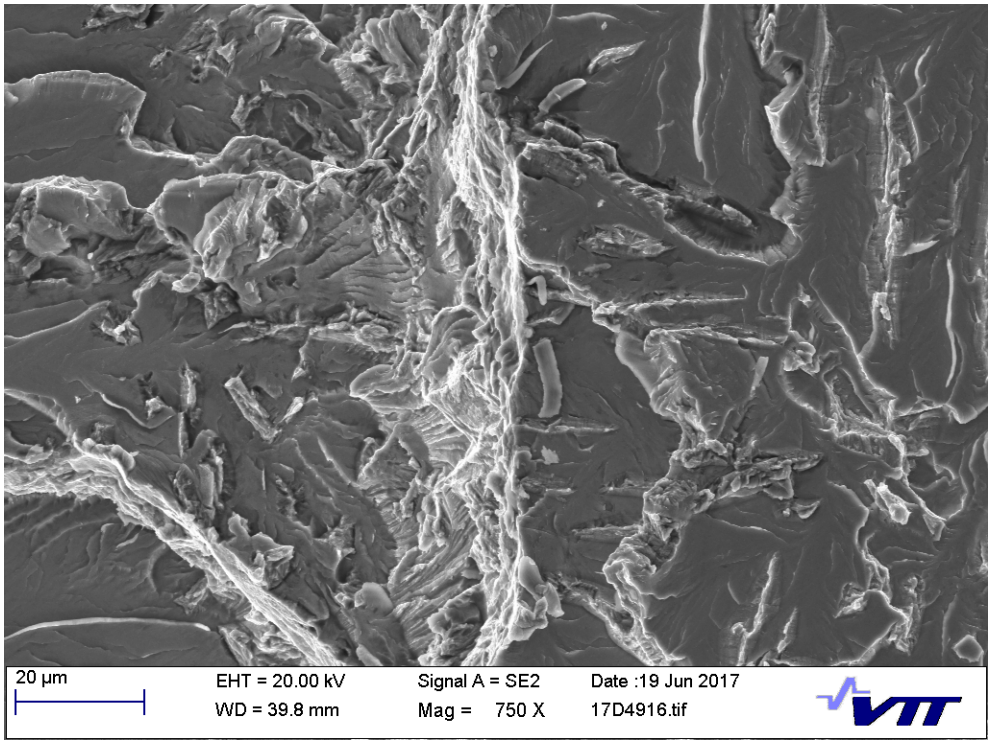

a)

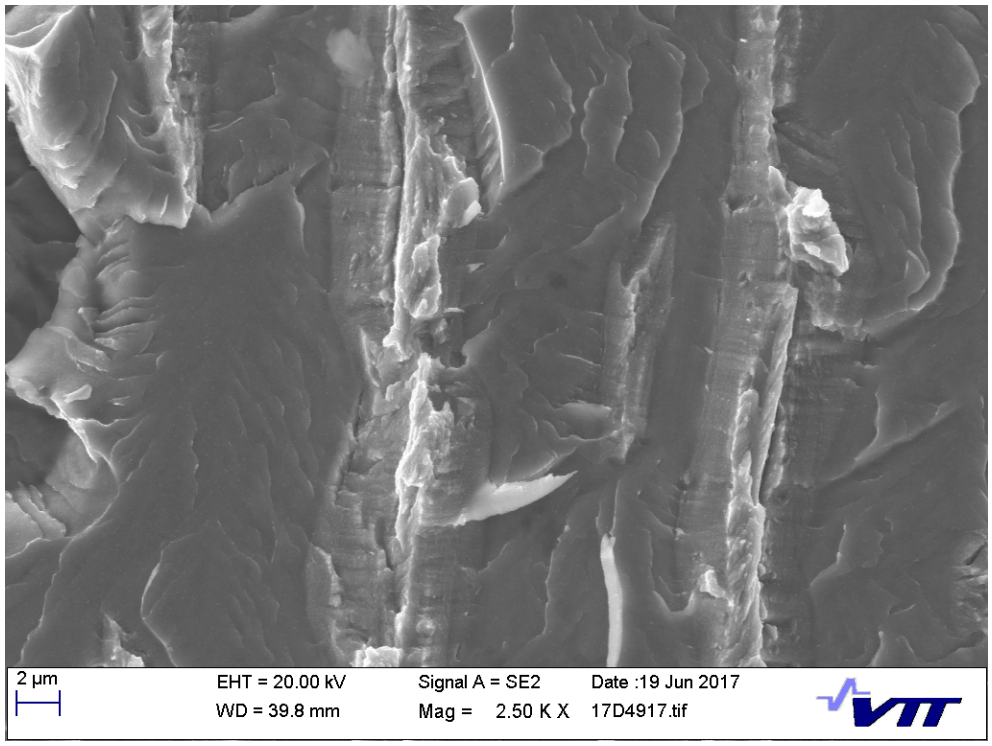

b)

Figure 4. Fracture surface from the middle of the sample, showing (a) ridges; (b) striations. Outer surface on top, fracture propagation from top to bottom.

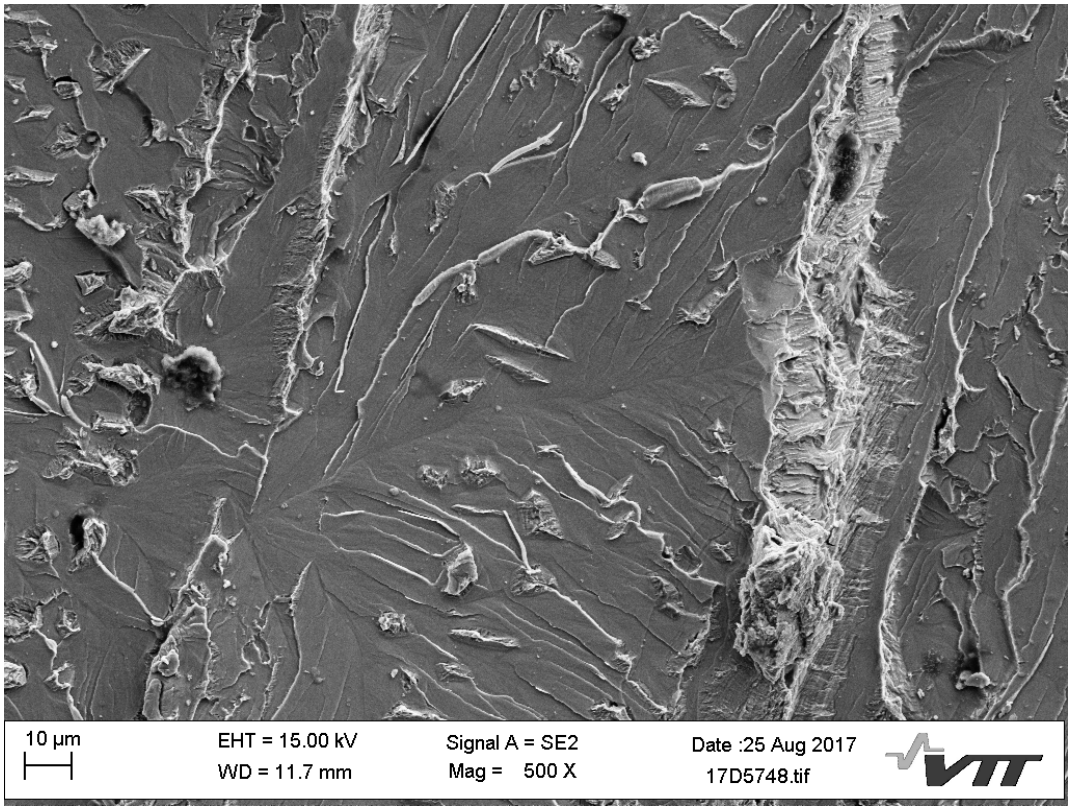

Figure 5. Fracture surface of the sample, showing features of “feathery” structure.

3.3 Metallographic investigation

According to the LOM microscopy of the cross section samples, the main cracks appeared very deep; they had propagated nearly through the entire section thickness (Figure 1). Several individual microcracks, of which one has grown to a main crack, were discovered on the plate outer surface (Figure 7). Various secondary microcracks, as well as pronounced crack branching and crack bridging were also found along the crack propagation path.

An abnormal “peppery” structure was observed as a thin layer immediately next to the plate surface and adjacent to the main crack. This anomalous structure presented coarse grain size composing of elongated side-plate/ lath-like austenite mainly in the ferrite grain boundaries and heavy intragranular precipitation within the ferrite phase (Figure 6). The depth of the anomalous structure varied from 80 to 200 µm, being ~90 µm at the crack initiation site (Figure 7).

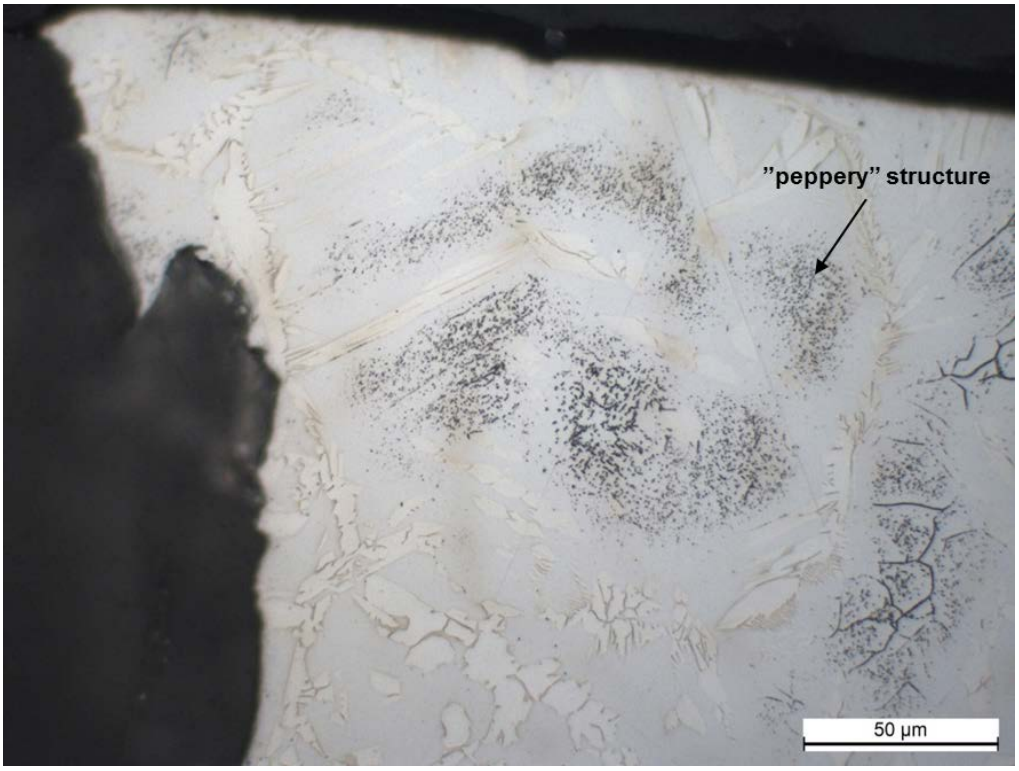

Figure 6. A thin abnormal layer next to the plate surface, adjacent to the main crack ("peppery" structure).

According to the LOM examination, the crack appearance and fracture morphology were identical with all the examined samples. The main cracks appeared rupture-like and very deep; they had propagated nearly through the entire section thickness (Figures 1 and 7). Apart from the main crack, individual microcracks were discovered at the plate outer surface (Figure 7). Secondary microcracks, as well as crack branching and crack bridging were also found along the crack propagation path (Figures 7 and 12).

Contrary to the uniform crack morphology, various abnormal, thin, local layers and structures were observed at, or next to, the surface of the gas separator samples close to the circumferential butt-welds. Of these, three slightly different types of anomalies were distinguished:

(i) A thin, whitish surface layer at the plate surface and adjacent to the circumferential butt-weld, which had etched very differently compared to the base material. Beneath this layer appeared a coarse-grained region resembling the heat-affected zone (HAZ) rather than typical duplex base material, by composing of elongated side-plate/lath-like austenite mainly in the grain boundaries of coarse ferrite grains (Figures 6 and 7).

(ii) A local anomalous 'rough' surface region adjacent to the circumferential butt-weld, which exhibited a coarse-grained region immediately beneath the plate surface, composing of elongated side-plate/lath-like austenite mainly in the grain boundaries of coarse ferrite grains that also revealed intragranular precipitation within the grain interiors (i.e. sc. "peppery" structure). This local microstructure resembled the HAZ rather than base material (Figures 8–10).

(iii) A local thin, anomalously deformed and partially torn-off 'alien' surface layer at the plate surface immediately adjacent to the circumferential butt-weld, with a typical parent steel duplex microstructure beneath it (Figure 11).

Figure 7. Crack initiation at the outer surface of the specimen close to the weldment, thin layer with "peppery" structure, several individual microcracks at the surface, crack branching along the propagation path.

Overall, quality of the circumferential butt-welds was poor; the welds reveal a vast number of both surface and internal imperfections and defects, such as (i) continuous weld undercut, (ii) incorrect weld toe, (iii) excessive weld metal, (iv) clusters of porosity, (v) occasional microcracks, (vi) lack-of-fusion defects and (vii) incomplete penetration (lack of penetration) in the weld root area. These weld deficiencies, however, were not in direct connection to the observed failure.

The microstructure of the base material and the weld metal consisted of a mixture of ferrite and austenite and was hence typical of duplex stainless steel. The microstructures also exhibited an appropriate balance between the ferrite and the austenite phases, approximately a ratio of 43/57 (Figure 13).

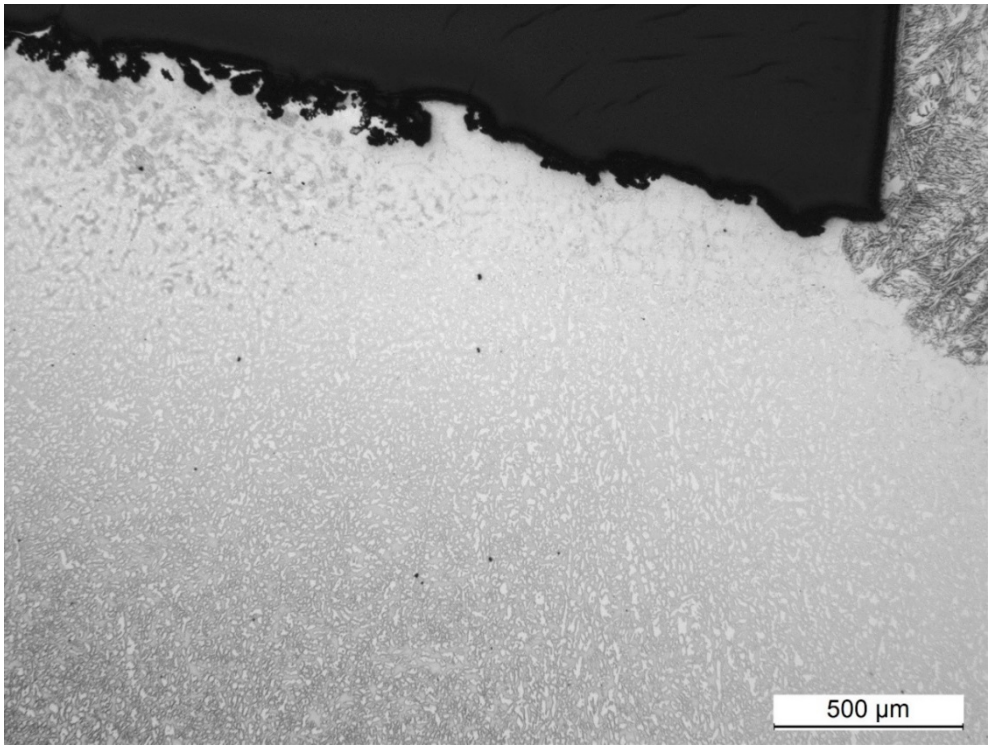

Figure 8. A local thin abnormal ‘rough’ surface layer (top, left) adjacent to the butt-weld (top, right).

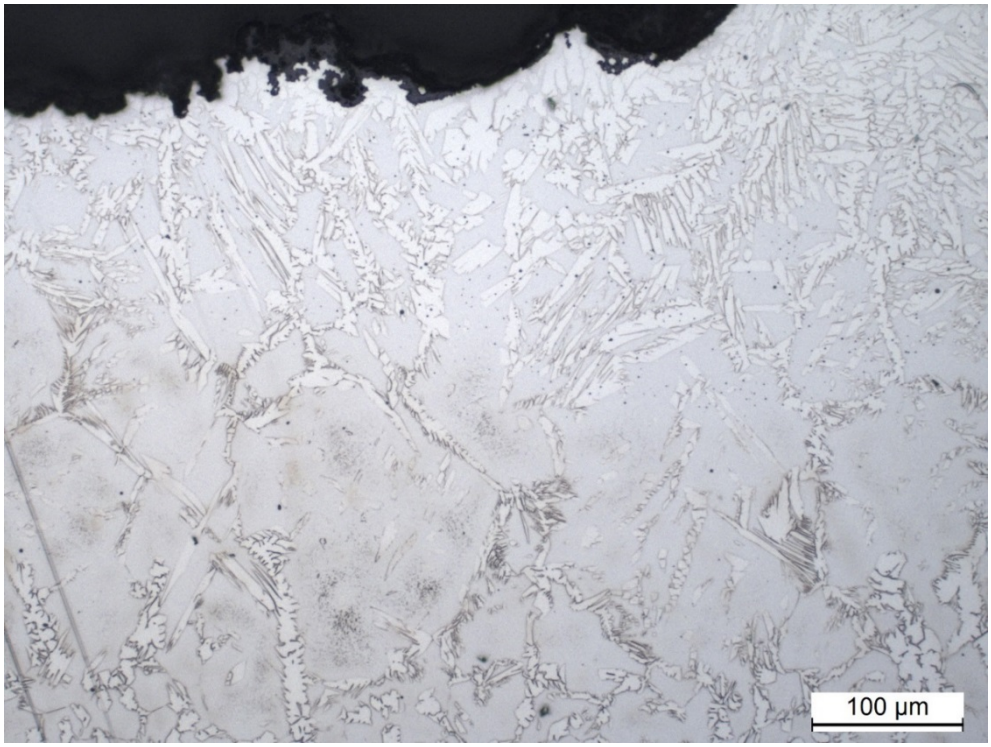

Figure 9. Detail from Figure 8. A local abnormal ‘rough’ surface layer adjacent to the circumferential butt-weld – grain-coarsened microstructure beneath the plate surface resembling the HAZ and composing of elongated side-plate/lath-like austenite mainly in the grain boundaries of coarse ferrite grains and traces of intragranular precipitation within the ferrite.

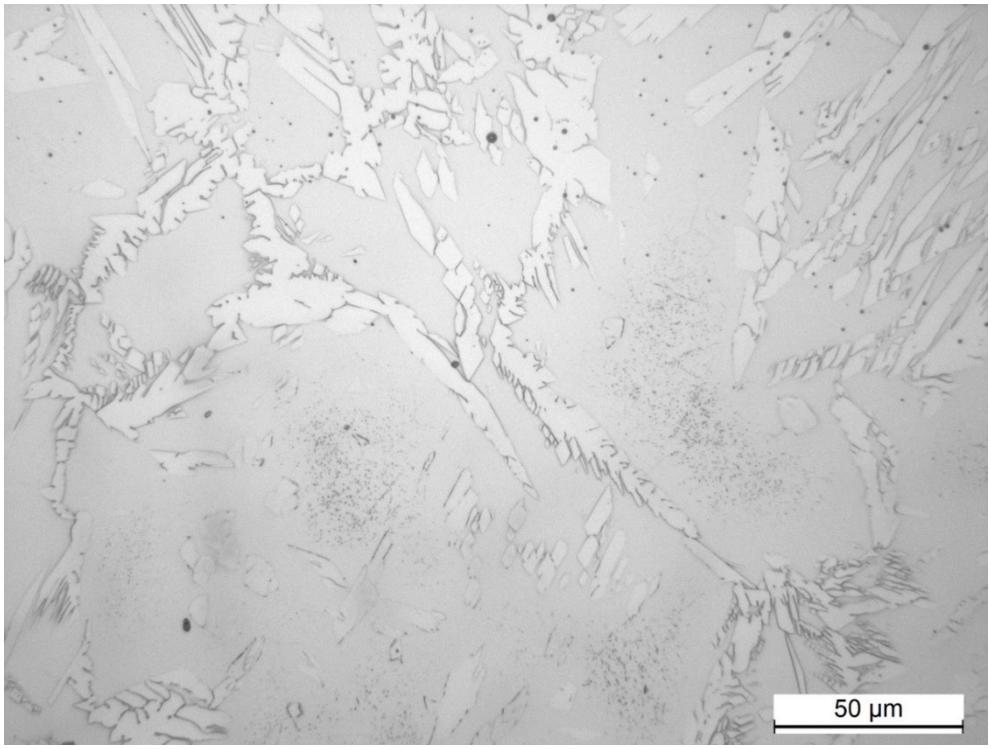

Figure 10. Detail from Figure 9. Coarse-grained microstructure beneath the abnormal ‘rough’ surface layer resembling the HAZ and revealing intragranular precipitation within the ferrite (“peppery” structure).

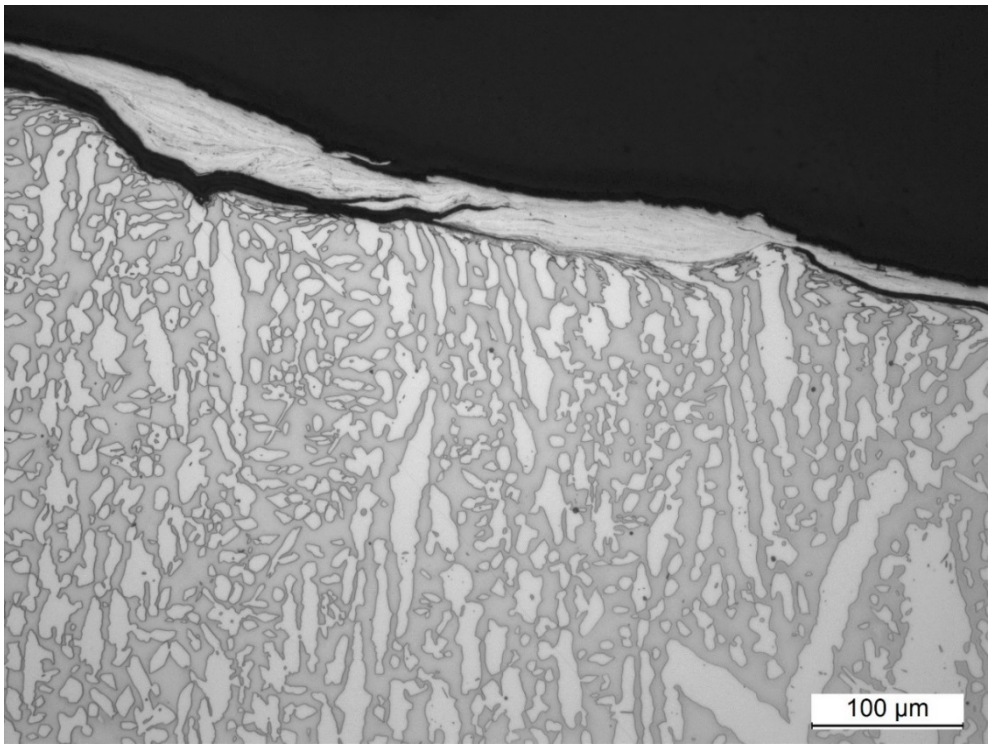

Figure 11. A local thin anomalous, deformed and torn-off surface layer (white) on the plate surface adjacent to the circumferential butt-weld, typical parent steel duplex microstructure beneath the surface layer.

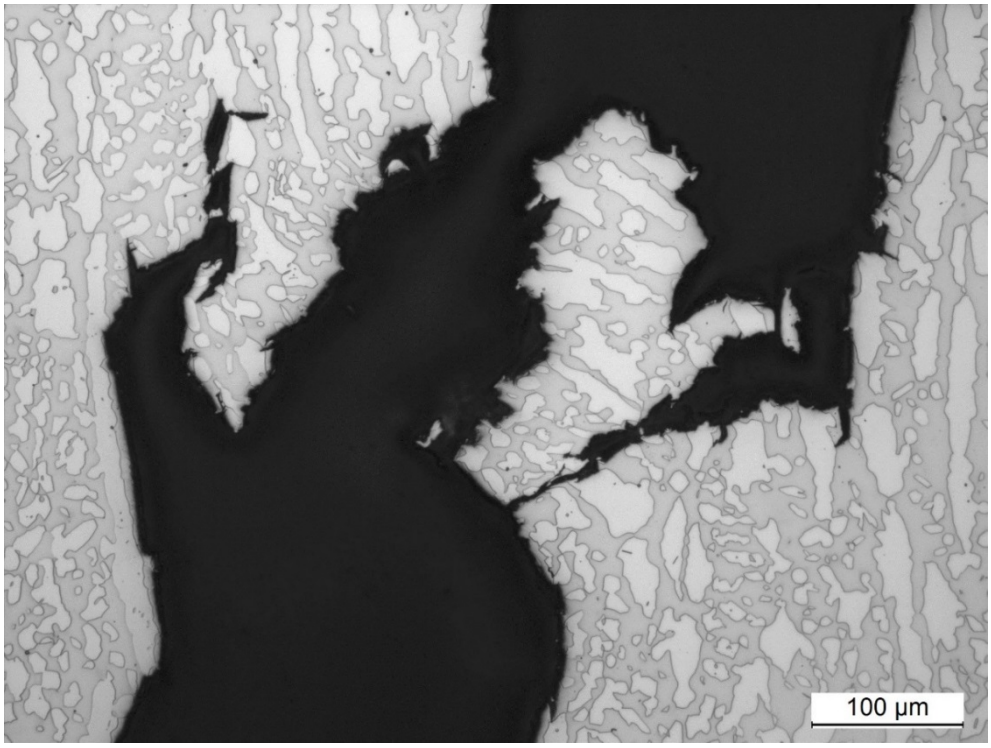

Figure 12. Crack propagation through the circumferentially welded gas separator specimen – propagation path mainly within the ferrite phase (grey) and circumventing the austenite phase (white).

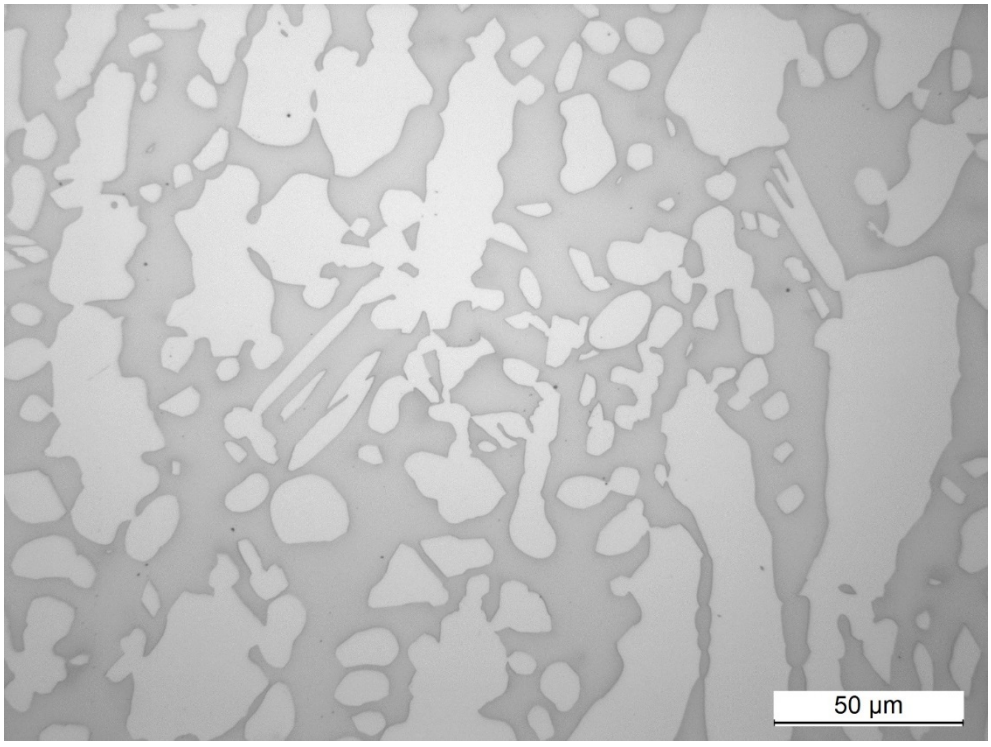

Figure 13. Microstructure of the base material; ferrite (grey), austenite (white).

3.4 Hardness measurements

The results of the hardness measurements on the investigated gas separator material, made in through-thickness direction of the plate, are given in Table 2.

According to the measurements, the hardness of the base material ranges from 220 to 295 HV, the average being around 265 HV, which is a typical hardness level for the 2205 grade duplex material. It is noteworthy that the hardness of a thin surface layer comprising an anomalous microstructure exhibits clearly higher hardness (317 HV) than either the ferrite or the austenite phase. No essential difference in the average hardness between the ferrite and the austenite phase was recognised.

Table 2. Results of the Vickers microhardness measurements of the gas separator material ($HV_{0.1}$).

Hardness / location	**Austenite**	**Ferrite**	**Surface layer** (depth of 0.1 mm from surface)
Average	268 ± 21	261 ± 7	317 ± 8
Maximum	295	269	326
Minimum	220	251	307

4. Discussion and Conclusions

According to the microscopic and fractographic investigations of the damaged gas separator specimens made of 2205 grade duplex stainless steel, the discovered cracks exhibited features typical of hydrogen-induced stress cracking (HISC) and subsequent fatigue failure. Previously reported failures occurring due to the HISC mechanism have usually been associated with duplex stainless steel for sub-sea components that are exposed to cathodic protection system acting as a source of continuous supply of hydrogen.

The following discovered features associated with the examined samples are regarded characteristic of the HISC mechanism, in particular:

(i) The existence of multiple individual surface microcracks close to the plate outer surface, immediately adjacent to the primary crack, acting as initiation sites for HISC (Figure 7).

(ii) The presence of intragranular Cr_2N precipitates and a coarse-grained microstructure within a thin layer next to the plate surface, promoting crack initiation via HISC (Figures 6, 9 and 10).

(iii) The presence of welded joint relatively close to the crack initiation region (Figures 1 and 8).

(iv) Crack location and propagation essentially within the ferrite phase via transgranular quasi-cleavage micromechanism, i.e., brittle-like fracture, with no indication of gross plastic deformation (Figures 2, 5 and 12).

(v) Associated secondary micro-cracking, crack branching and crack bridging near a growing primary crack as it propagates further (Figures 1, 6, 7 and 12).

(vi) The propagating cracks typically tend to circumvent the austenite phase, rather than grow within or across it (Figure 12)

(vii) When cracks did propagate in the austenite, the associated fracture mode was ductile tearing, i.e. ductile overload (Figure 3).

(viii) The macroscopically straightforward growth direction, as well as a torn, rupture-like appearance of the discovered main cracks imply an involvement of heavy stress state, which most likely accrues from excessive welding residual stresses due to heavy restraint and rigidity of the gas separator component (Figures 1, 6 and 7).

(ix) Continuous supply of large amounts of hydrogen from the flowing content of the gas separator and, possibly, local pitting corrosion reactions on the plate surface (Figure 8).

In general, duplex stainless steels are considered resistant to *hydrogen cracking*. Environmentally assisted hydrogen cracking in duplex steel has been attributed primarily to poor microstructure control, i.e., distorted ferrite-austenite balance deviating from the 50–50 ratio in terms of excessively high ferrite content equal to or beyond approx. 70% (FN > 80) [1,3,4]. Based on the microscopic investigation, it is clear that this is not the case in the present study, as microscopy showed more or less appropriate 43–57 ferrite-austenite ratio in the parent steel both around and in front of the crack propagation path (Figures 12–13). Only within a thin layer next to the plate surface where the cracks had initiated, excessively high ferrite content was occasionally recognised; the microstructure consisted of large ferrite grains with intragranular precipitates and only some austenite mainly in the grain boundaries (Figures 9–10). According to literature, it appears that particularly the *hydrogen-induced stress cracking (HISC)* mechanism can occur in, and has been found in the case of, duplex microstructures that contain acceptable balance of ferrite and austenite. An excessively high ferrite content therefore seems not to be a prerequisite to the occurrence of the HISC in DSS, provided other critical factors, such as high stress state and continuous supply of hydrogen, prevail.

A crucially important factor promoting crack initiation in the examined samples is obviously the presence of *local anomalous microstructures* within a thin layer next to the plate surface and close to the individual surface cracks (Figures 6, 7, 9 and 10). It consists of a phase morphology rather resembling the HAZ than base material in the sense that the grain size is coarsened, and the austenite phase has elongated to resemble a side-plate/lath like structure decorating and delineating the primary-ferrite grain boundaries. The ferrite grain interiors show only small amount of austenite. Significant amounts of precipitates are recognised within the ferrite phase resembling classical intragranular “peppery” structure (Figure 10) typical of e.g. ferritic stainless steel HAZ [1] and consisting of chromium nitrides, Cr_2N, precipitated during fast cooling after prior heating stage. It is also noteworthy that this thin surface layer exhibited hardness clearly higher than that associated with either the ferrite or the austenite phase alone (Table 2). The presence of intragranular Cr_2N precipitates and coarse-grained microstructure have been attributed to an increased susceptibility to hydrogen embrittlement and a degradation of the HISC resistance of the duplex material [1]. There exists evidence that the Cr_2N precipitates induce a detrimental effect on the HISC resistance via their ability to lower the net section stress at failure, i.e., they impair the mechanical properties of the duplex microstructure under external loading conditions. This effect is further aggravated by the presence of hydrogen and subsequent transportation of diffusible hydrogen to areas with tri-axial stresses, such as weld toe.

The somewhat complex nature and variety of *local anomalous surface regions* among all the examined samples complicates the analysis of the origin and significance of these anomalies. Firstly, the spectrum of abnormalities was wide since not all the anomalies were associated with HAZ-resembling microstructures; for instance, some samples revealed heavily deformed, partly torn-off surface abnormality close to the circumferential butt-weld, which was associated with typical duplex steel base material microstructure (Figure 11). Secondly, there were cases of surface abnormality associated with HAZ-resembling microstructures both with cracks initiated at the plate surface (Figures 6, 7, 9 and 10) and without any initiated cracks (Figure 8), as well as initiated cracks without a concomitant presence of surface abnormalities (Figure 12). These findings suggest that the presence of these local, thin anomalous surface, or next-to-surface, regions can assist crack initiation, but their existence alone will not lead unavoidably to crack initiation. It is also obvious that crack initiation at the plate surface in the present case can also occur without the presence of any anomalous local region, at least when the initiation site is at the weld toe with obviously high local stress concentration.

The underlying causes for the aforementioned *anomalous local surface layers/regions* remained unexplained, as, after all, they were not uniform in nature and, in most cases, situated too far away from the circumferential butt-weld to be a result of the weld thermal cycles associated with it. Nevertheless, the fact that the existence of ‘rough’ surface abnormality clearly was accompanied by the HAZ-resembling microstructure instead of base material microstructure can be regarded as an inevitable indication of incidental thermal exposure in some stage of welding fabrication. Such exposure can be a consequence of accidental inappropriate thermal-mechanical treatment during the installation assembly work, originating from e.g. plasma cutting, flame straightening, fitting by force or deposition of temporary attachment welds that had been later removed.

No essential difference in the average *hardness* between the ferrite and the austenite phase of the base material was recognised (Table 2). Therefore, it was not possible to conclude based on hardness, whether any high-temperature embrittlement had occurred in the ferrite during the welding fabrication. The micros-

copy revealed no evidence of the presence of any *brittle metallic phases*, such as sigma phase. The discovered internal volumetric *imperfections within the weld metal* close to the weld root region (c.f. Figure 1) imply that welding of the root had technically failed in this respect; however, the weld metal defects were not in direct connection to the observed failure and are hence of secondary importance in this sense.

Literature on *hydrogen damage* reports that sc. "feathery" structure on the fracture surface accompanied by cleavage-like cracking macroscopically parallel to {100} crystallographic planes in <110> directions, with extensive slip on {111} planes intersecting transgranular cracks, has been attributed to sc. AIDE (Adsorption Induced Dislocation Emission) mechanism [5]. An example showing features of such "feathery" structure on the cleavage-like crack fracture surface in the present duplex material is given in Figure 5. The AIDE mechanism is one of the three postulated main micromechanisms associated with hydrogen-assisted cracking [5]. The features in Figure 5 can therefore be regarded as further evidence of the decisive role of hydrogen in inducing the crack initiation and assisting crack propagation in the present case. Since the examples given in the literature [5], however, were frequently associated with metallic materials other than duplex steel, the existence of the AIDE mechanism in the present case cannot be solely confirmed, nor excluded.

That the fractography revealed *local areas with striations* on the crack fracture surfaces, oriented perpendicular to the crack growth direction (Figure 4b), is considered somewhat unexpected. According to the customer, there should not have been such variable loads during the operational period of the present gas separator that are expected to cause any fatigue damage. The observed striations were therefore examined carefully, in order to rule out the possibility that they in fact could have been some kind of ridges caused by stepwise propagation of cracks provoked by the HISC mechanism. It is worth pointing out that a possibility of confusing between fatigue-associated striations and stepwise ridges caused by the HISC mechanism has been addressed in the literature. The authors opinion, however, is that the discovered features on the fracture surfaces in the present case are truly striations and, hence, an indisputable evidence of fatigue failure mechanism that has occurred at later stages of the crack propagation. Apart from striations, *ridges* were also discovered on the crack fracture surfaces (Figure 4a); however, the appearance of ridges clearly relates to a different scale of fractographic details; compare Figures 4a and 4b.

Consequently, it is thereby concluded that the present failure mechanism in the investigated 2205 duplex gas separator material has been a combination of (i) *hydrogen-induced stress cracking (HISC)* and later (ii) *fatigue damage*, where the crack initiation and subsequent propagation have firstly occurred via the HISC mechanism, followed by later propagation stages contributed by the fatigue mechanism.

References

1. J.C. Lippold & D.J. Kotecki (2005), Welding Metallurgy and Weldability of Stainless Steels, John Wiley & Sons, Inc., Hoboken, New Jersey, U.S.A. Wiley Interscience. First Edition. 357 p.

2. American Petroleum Institute (2011), Use of Duplex Stainless Steels in the Oil Refining Industry, Downstream Segment, API Technical Report 938-C, Second Edition, April 2011.

3. L. Karlsson (2012), Welding Duplex Stainless Steels - A review of Current Recommendations, Welding in the World 56 (2012) 05/06. pp. 65-76.

4. A. Kyröläinen & J. Lukkari (1999), Ruostumattomat teräkset ja niiden hitsaus, Metalliteollisuuden keskusliitto (MET), Metalliteollisuuden Kustannus Oy, Helsinki, Finland. 530 p. (in Finnish)

5. S.P. Lynch (2003), Mechanisms of Hydrogen-Assisted Cracking - A Review, In: Hydrogen Effects on Material Behavior and Corrosion Deformation Interactions. Eds. N.R. Moody, A.W. Thompson, R.E. Ricker, G.W. Was and R.H. Jones. The Minerals, Metals & Materials Society (TMS) 2003. pp. 449–466.